GEM TN-93-394

First Level Trigger in the GEM Muon System

Y.P. Dingus, H. Uijterwaal, Ya-Nan Guo
Physics Research Department
Superconducting Super Collider Laboratory

July 16, 1993

Abstract:

The GEM first level muon trigger efficiency was determined by scanning the GEM detector with 48000 single muons in six bins of P_t; 5, 10, 20, 30, 40, and 70 GeV. The distribution of trigger strips corresponding to the track "three point" $\Delta\phi$ was then used to compute the trigger efficiency as a function of preset trigger P_t thresholds. We then convoluted these efficiencies with the charged particle punchthrough rates as a function of η and P_t in order to get the GEM first level muon trigger rates. This algorithm was later incorporated into the GEMFAST parameterized simulation[1] and used to compute the trigger probabilities for various physics processes in the GEM TDR.

First Level Trigger in the Gem Muon System

P. Dingus, H. Uijterwaal, Ya-Nan Guo
Physics Research Department
Superconducting Super Collider Laboratory
Dallas, TX 75237

Abstract: The GEM first level muon trigger efficiency was determined by scanning the GEM detector with 48000 single muons in six bins of P_t; 5, 10, 20, 30, 40, and 70 GeV. The distribution of trigger strips corresponding to the track "three point" $\Delta\phi$ was then used to compute the trigger efficiency as a function of preset trigger P_t thresholds. We then convoluted these efficiencies with the charged particle punchthrough rates as a function of η and P_t in order to get the GEM first level muon trigger rates. This algorithm was later incorporated into the GEMFAST parameterized simulation[1] and used to compute the trigger probabilities for various physics processes in the GEM TDR.

1 Introduction

The trigger simulation was designed using the Sigem GEM monte carlo, which was also used in the simulation of the muon reconstruction efficiency [2] and in most detailed studies found in the GEM TDR (Technical Design Report). The Sigem monte carlo has been discribed elsewhere[3] but it should be mentioned here that it is an up-to-date representation of our Baseline II detector with a very detailed discription of the muon system including support structures, the correct magnetic field map and even $17\mu m$ copper strips in the CSC chamber readout. A schematic of the measurement primitives for both the "three point" $\Delta\phi$ and sagitta measurement techniques are shown in figure 0. We will adopt the convention that a muon chamber is the measurement unit consisting of a gas-gap readout and its associated hexcel support, while a superlayer is a collection of chambers (6 in both the barrel and endcap except for the first endcap superlayer which has 8 chambers).

[1] T.Skwarnicki, GEM Technical note in preparation.
[2] GEM-TN-93-387, Pattern Recognition in the GEM Muon System.
[3] Y.Fisyak GEM-TN-162

The level 1 trigger simulation was modeled on a $\Delta\phi$ variable which was shown to be correlated to the P_t of a charged track in both the barrel and endcap muon systems. The actual trigger primitive was expanded to include muon hits from all three superlayers so as to decrease the number of false triggers due to uncorrelated charged chamber hits thus achieving a trigger rate commensurate with our trigger budget even at low P_t threshold.

2 Digitization

An important aspect of any triggering scheme that one proposes is the jitter in the position of a charged hit due to the digitization process. As can be seen in figure 1, that a typical muon incident on the CSC chamber at $\phi \sim 90^0$, where ϕ is the angle between the muon track and the anode wire in the chamber, will have an induced charge distribution which spans several readout strips. The approximate charge distribution for a muon falling exactly in the center of a 0.5cm strip is about 80% of the charge is induced on the strip below the track and $\sim 10\%$ is induced on the two neighboring strips on either side. If, on the other hand, one averages the position of the muon, in the bend plane direction, over the entire strip width one finds that, on average, 65% of the charge is induced on that strip. This is, of course, the ideal case of normal incidence, in reality there is a uniform distribution of incidence angles for muons on chambers of $|\phi| \leq 4^0$ which translates into $\pm 7\%$ of a 0.5cm strip, thus the approximation of normal incidence is not unrealistic.

The hardware assumption made for the first level trigger is that the actual signal coming from a chamber strip is an on/off pulse that is the result of discriminating the charge on a strip at some level. Various proposals have been made[4]; such as setting the discriminator level at $\frac{Q}{4}$, where Q is the charge induced on a strip corresponding to the most probable value of the induced charge distribution. The conservative assumption made in this analysis is that if a hit is registered on some chamber strip, a gaussian random number is generated and scaled such that $\sigma = 0.5 \times (stripwidth)$ (in the bend direction). This random displacement, which is truncated to half a strip width if it exceeds that value, is added to the position of the muon hit, in the direction of the smallest fraction of the strip from the position of the hit to the next strip in the bend plane. Once this offset is made, the strip, which this position corresponds to, is taken as the discriminated strip centroid. Note, from figure 1, that at the $0.5 \times (stripwidth)$ the amount of charge induced on the neighboring strip is about 46% of the total charge.

The CSC strips, for the purpose of the trigger performance study, have been staggered by half strip widths on successive layers of a superlayer. Once a set of chambers have registered hits in a superlayer, the following algorithm is implemented:

[4]V.Balugura SSCL, GEM TN-93-404

- There must be at least 4 registered chambers out of 6 (or 8 on the first superlayer in the endcap) to qualify as a track segment. We make the assumption here that in the real trigger algorithm clusters will have been found and real track segments will have been distinguished from background random hits to some high efficiency[5].

- Only the first and fourth registered strips are used to establish the trigger centroid on the current superlayer. This centroid is then associated with the superlayer trigger tower.

3 Trigger Roads and Primitives

Once a set of trigger towers, one on each superlayer, has been registered the determination of a associated P_t was made. This can be done in two ways:

- $\Delta\phi$ road. This is done by establishing the correlation between muon tracks of known P_t, distributed over the entire muon spectrometer, and some variable giving the bend of the track in the ϕ direction (bend plane). The variable that was selected in this study was formed by first connecting the trigger tower on the first superlayer to the IP, and using this "infinite momentum" track to register virtual hits on each of the superlayers. We then took the actual hit trigger towers on the second and third superlayers and counted the number of strips between the virtual strip and the actual strip. If we designate the number of strips between the virtual and actual hits on the second superlayer by $N_{1,2}$ and that on the third superlayer by $N_{1,3}$, the $\Delta\phi$ road variable is $\Delta\phi = |N_{1,3} - N_{1,2}|$. Uniform scans over the entire GEM muon spectrometer for P_t's = 10, 20, 30, 40 GeV are shown in figure 2 for the averge $\Delta\phi$ as defined above.

- Sagitta road. The following formula establishes the sagitta:

$$\delta = |(\vec{h_3} + \vec{h_1})\frac{RZ_{2,3}}{RZ_{1,2} + RZ_{2,3}} - \vec{h_2}| \tag{1}$$

  where δ is the sagitta, h_n is the bend plane postion vector of the trigger tower on plane n, and $RZ_{m,n}$ is the distance, normal to the measurement planes, between planes m and n. The sagitta is the deviation on the second superlayer of the registered trigger tower from the position given by the intercept, on the second superlayer, of the cord joining the first and third superlayers. The sagitta is related to the P_t as follows:

$$\delta(mm) = \frac{0.3B(Tesla)l^2(m)}{8P_t(\frac{TeV}{c})} \tag{2}$$

[5]GEM-TN-93-387, Pattern Recognition in the GEM Muon System.

Uniform scans over the entire GEM muon sepectrometer for P_t's between 10 GeV and 40 GeV are shown in figure 3.

The sagitta method was found to have a bad dynamic range for high P_t tracks. The difference in the average number of strips characterizing the trigger road between 20 and 30 GeV P_t is 1. This 1 strip separation is for a percise centroid calculation of the sagitta. If the digitization algorithm of section 2 is applied one sees a $\sim 10\%$ ambiguity (overlap) of the two trigger roads and $\sim 10\%$ spills out into the one strip bin. This is shown in figure 4.

The "three point" $\Delta\phi$ method has been found to be robust for P_t's between 5-70 GeV inclusive over the entire η coverage of the detector. The separation in the distribution of trigger roads for different P_t's is good as can be seen in figures 5 and 6; but the widths of these roads (the width in the distribution of the number of strips associated with a given P_t) are large compared to those given if the sagitta algorithm is used. This in turn would give a larger number of false triggers than the sagitta method. For this reason, we impose the added constraint on the $\Delta\phi$ road of a hit on the first superlayer that is consistant with a track corresponding to at least the P_t threshold set in the trigger. For a P_t threshold set at 10 GeV (i.e. we wish to trigger on tracks with $P_t \geq 10GeV$), and assuming an occupancy of 0.6% per strip for random charged hits with a charge integration time of 600ns; the constraint of a corresponding trigger tower on the first superlayer decreases the probablity of false triggers by a factor of 14 in the barrel and a factor of 6 in the endcap, the difference being that there are 6 planes in the first superlayer of the barrel and 8 for the first superlayer of the endcap.

4 Trigger Efficiency

The trigger efficiency was calculated using the "three point" $\Delta\phi$ algorithm. It was implimented by taking the set of single muon scans over the GEM muon spectrometer and using the average values and distribution widths as a function of P_t to establish a P_t threshold on the trigger. For the isolated muon scans, uniform in η for several P_t's, we established tables corresponding to the average value of the number of strips, $\Delta\phi = |N_{1,3} - N_{1,2}|$, and the widths, in $\pm strips$, associated with 10 η bins and 8 P_t bins. We then used these tables, by interpolation, to determine whether the trigger primitive calculated for a track under consideration would yield a trigger. The track under consideration must always be one that has passed all the requirements imposed by the "road test" discussed earlier.

The trigger efficiency was tuned so as to yield a trigger if the $\Delta\phi$, in strips, for the current track was $\geq 1\sigma$ below the average value of the trigger primitive for the trigger threshold. Note that if the $\Delta\phi$, for the current track, is larger than that of the average

trigger threshold the P_t is less than that of the threshold, i.e. a smaller P_t corresponds to a greater bend and thus a greater number of strips. With this setting we find that 50% of tracks with a P_t equal to that of the trigger threshold are accepted and, due to the 1σ criterion, 34% of the tracks, with a $\Delta\phi$ number of strips below the average value of the trigger threshold, would also be accepted if the distribution of pads at the trigger threshold were gaussian. This is certainly the case as was seen in figures 5 and 6. Thus the efficiency is tuned to accept 84% of the tracks at the trigger threshold. This can be seen in figures 7 and 8, which show the trigger efficiencies for the barrel and the endcap muon systems respectively.

Barrel Trigger Threshold							
10 GeV		20 GeV		30 GeV		40 GeV	
P_t	Prob	P_t	Prob	P_t	Prob	P_t	Prob
6.0	0.0	9.0	0.0	13.0	0.0	14.0	0.0
7.0	0.001	10.0	0.001	14.0	0.005	15.0	0.002
8.0	0.0149	11.0	0.007	15.0	0.131	16.0	0.007
9.0	0.1986	12.0	0.021	16.0	0.031	20.0	0.073
10.0	0.7725	13.0	0.072	17.0	0.061	30.0	0.459
11.0	0.9547	14.0	0.127	18.0	0.102	40.0	0.846
12.0	1.0	15.0	0.323	19.0	0.172	50.0	0.947
13.0	1.0	16.0	0.445	20.0	0.265	53.0	0.956
14.0	1.0	17.0	0.546	30.0	0.840	54.0	0.964
15.0	1.0	18.0	0.674	31.0	0.859	55.0	0.970
16.0	1.0	19.0	0.757	34.0	0.931	56.0	0.971
17.0	1.0	20.0	0.855	35.0	0.951	57.0	0.972
18.0	1.0	21.0	0.881	36.0	0.955	58.0	0.978
19.0	1.0	22.0	0.942	37.0	0.968	59.0	0.978
20.0	1.0	23.0	0.959	38.0	0.976	60.0	0.980
21.0	1.0	24.0	1.0	39.0	1.0	61.0	1.0

Endcap Trigger Threshold							
10 GeV		20 GeV		30 GeV		40 GeV	
P_t	Prob	P_t	Prob	P_t	Prob	P_t	Prob
4.0	0.0	4.0	0.0	6.0	0.0	6.0	0.001
5.0	0.034	5.0	0.002	7.0	0.003	7.0	0.003
6.0	0.098	6.0	0.010	8.0	0.008	8.0	0.003
7.0	0.179	7.0	0.020	9.0	0.014	9.0	0.003
8.0	0.317	8.0	0.044	10.0	0.028	10.0	0.004
9.0	0.585	9.0	0.127	20.0	0.392	20.0	0.140
10.0	0.795	10.0	0.087	30.0	0.824	30.0	0.498
11.0	0.904	11.0	0.127	31.0	0.846	40.0	0.825
12.0	0.950	20.0	0.840	32.0	0.857	50.0	0.937
13.0	0.971	21.0	0.850	33.0	0.885	55.0	0.955
14.0	1.0	22.0	0.916	34.0	0.920	56.0	0.957
15.0	1.0	23.0	0.925	35.0	0.940	57.0	0.966
16.0	1.0	24.0	0.954	36.0	0.945	58.0	0.976
17.0	1.0	25.0	0.979	37.0	0.956	59.0	0.978
18.0	1.0	26.0	0.980	38.0	0.978	60.0	0.980
19.0	1.0	27.0	1.0	39.0	1.0	61.0	1.0

5 Trigger Rate

In order to calculate trigger rates using the "three point" $\Delta\phi$ trigger algorithm we used a data set prepared by one of our collaborators [6]. The data set was generated by using ISAJET TWOJET[7] events and then passed through a Geant based code which simulated the depth, in interaction lengths, of the GEM detector as a function of η. This was essentially the same simulated data presented for the calorimeter-depth studies used in the GEM TDR. The punchthrough rate as a function of P_t was convoluted with a trigger efficiency parameterization to yield trigger rates in four η regions of the spectrometer, and a total integrated rate as a function of P_t, as can be seen in figures 9 and 10 respectively. Charged tracks made available to the trigger by this data set include prompt muons, muons from $\pi\backslash K$ decays, and hadronic punchthrough. The trigger rates for a luminosity of $10^{33} cm^{-2} sec^{-1}$ are given in the table below at several different P_t thresholds.

[6] R.McNeil."PCHTHR"-A Fast Simulation for Hadron Punchthrough, GEM TN-92-193.

[7] F.E.Page and S.D.Protopopescu, "ISAJET", BNL-38774(1986).

Trigger Rates in Hz				
P_t GeV	10	20	30	40
η				
0.1-0.5	532.5	124.8	48.5	22.9
0.5-1.0	483.9	130.9	47.1	22.8
1.0-1.5	643.1	152.3	62.0	28.8
1.5-2.0	1167.8	263.7	105.9	47.7
2.0-2.5	1057.8	247.8	102.5	43.8
Sum	3885.1	919.6	365.9	166.0

6 Conclusion

The GEM first level trigger rate, for the whole detector, has been given an upper limit of 100kHz[8]. A soft target for the muon first level trigger rate has been set at $\leq 10kHz$. The performance of the "three point" $\Delta\phi$ trigger algorithm has been found to be well within this target. As can be seen, from the table above, we find the integrated muon trigger rate, from two-jet QCD events, to be $\leq 4kHz$ for a trigger threshold of 10 GeV.

[8]GEM TDR

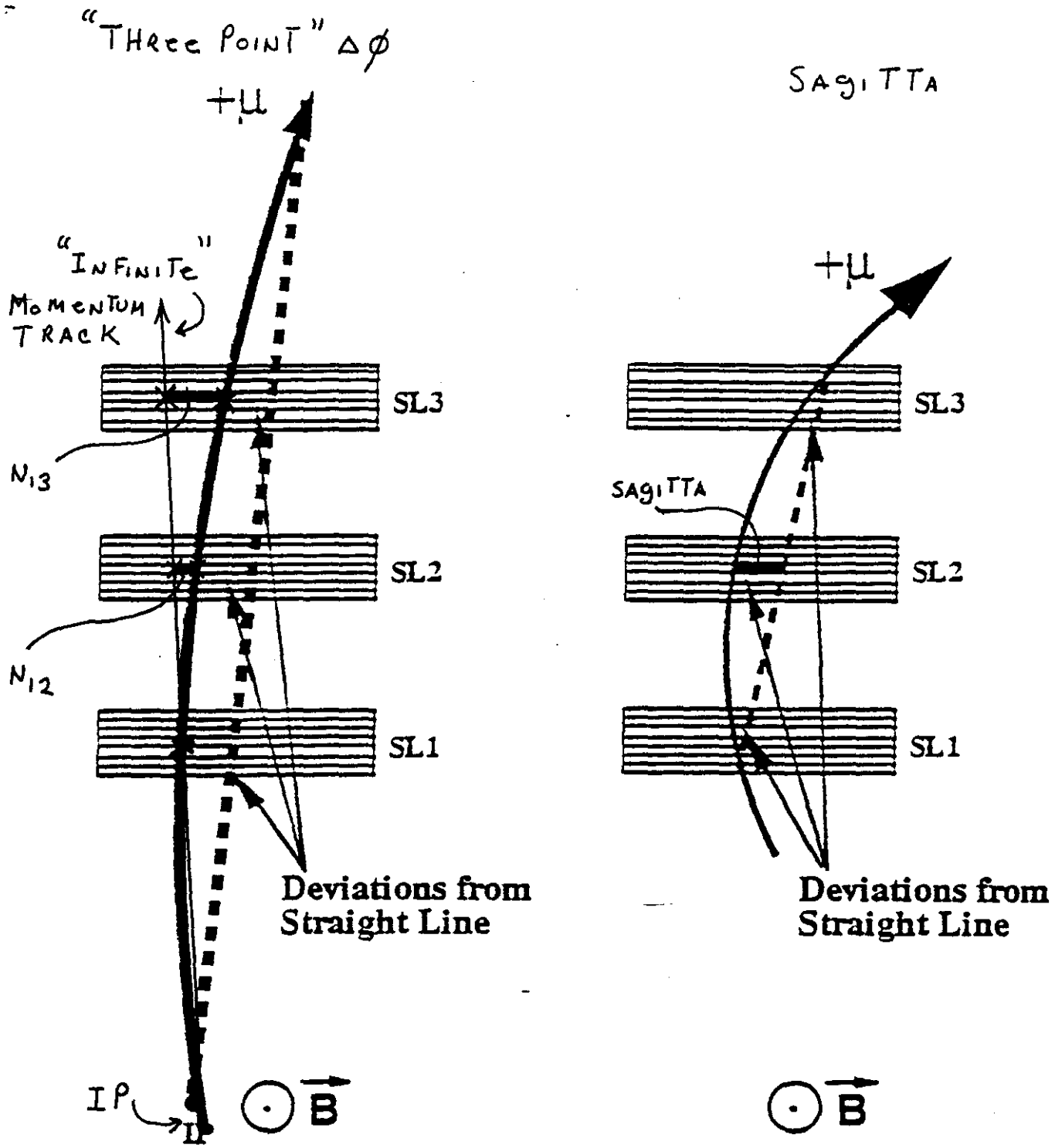

Figure 0) (a) Three point $\Delta\phi$ trigger primitive (b) Sagitta trigger primitive .

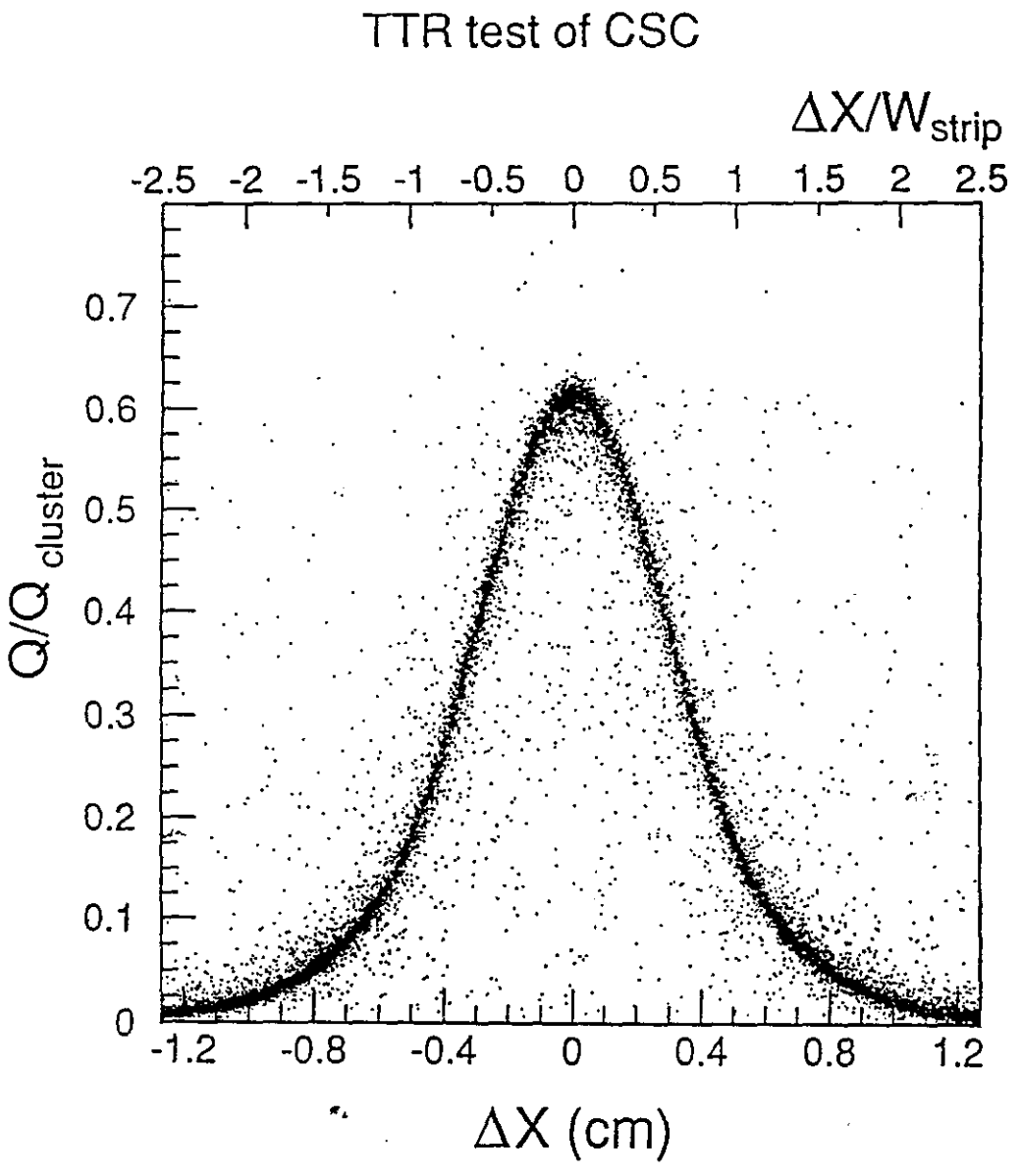

Figure 1) Charge distribution for 0.5cm strips from TTR test of CSC chamber. Plot taken from GEM TN-93-404 p87.

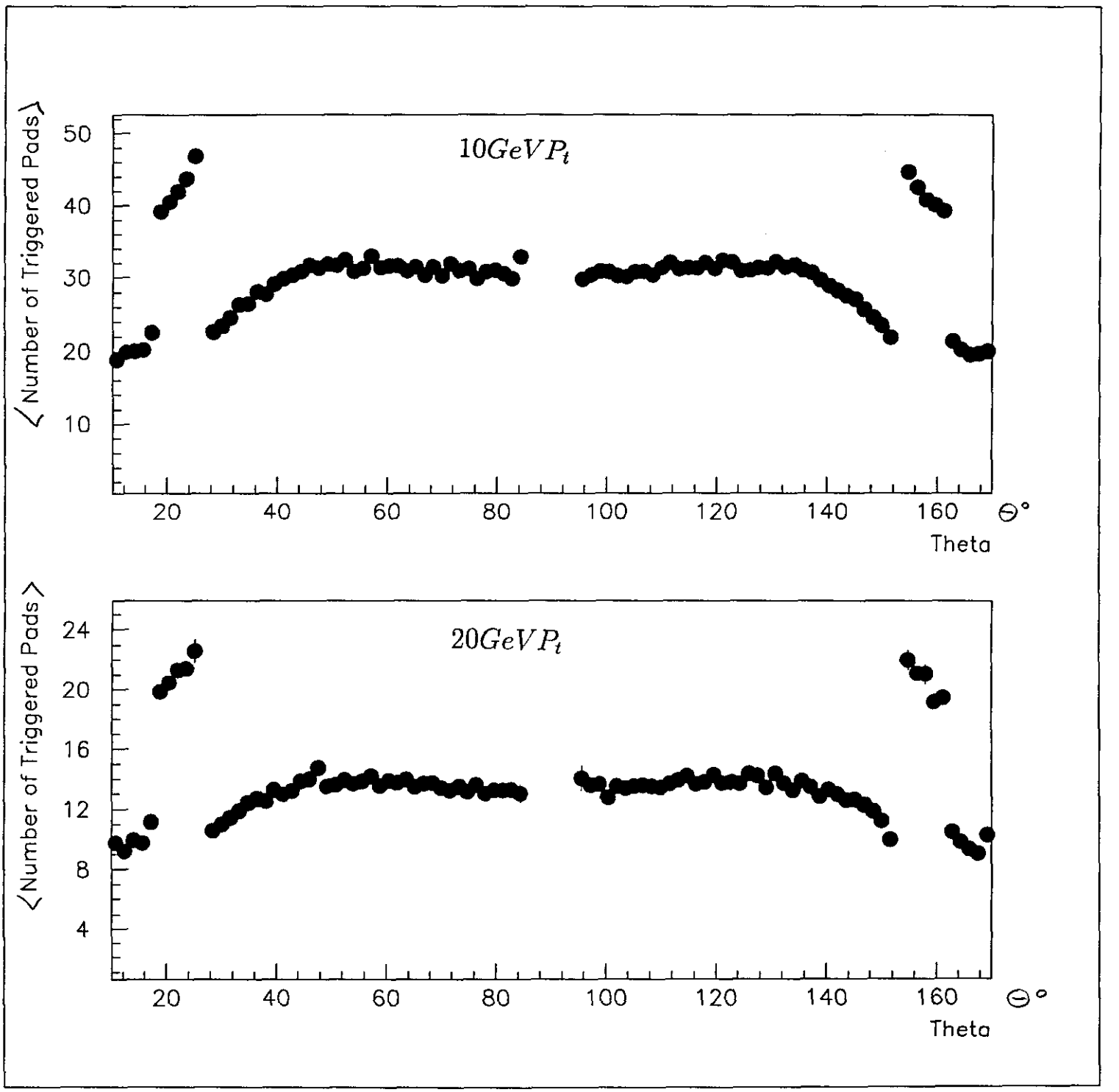

Figure 2a) Scan of the average value of the distribution of strips for the "three point" $\Delta\phi$ determination of a trigger road as a function of θ. These distributions are for a constant P_t of 10 and 20 GeV. .

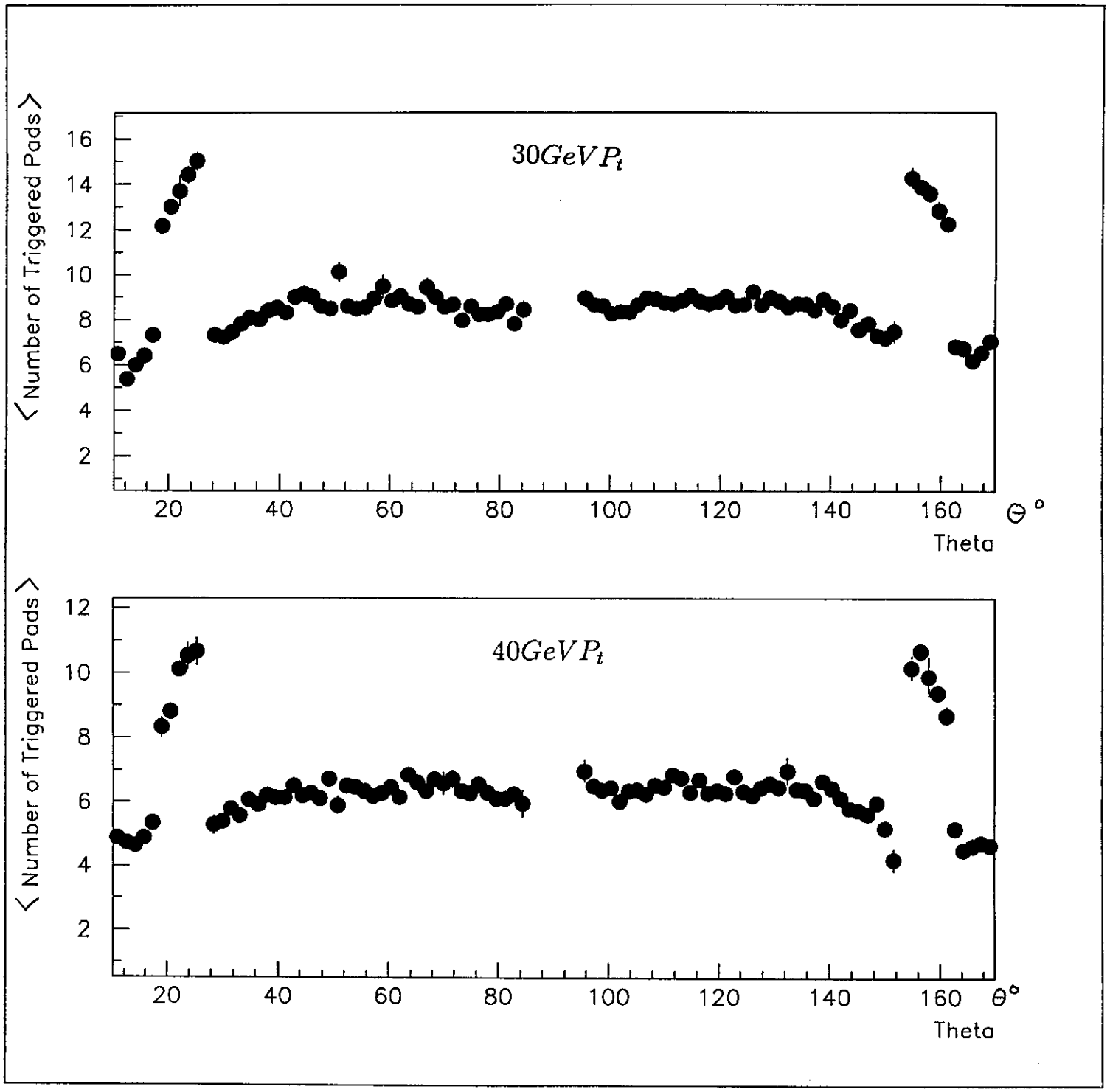

Figure 2b) Scan of the average value of the distribution of strips for the "three point" $\Delta\phi$ determination of a trigger road as a function of θ. These distributions are for a constant P_t of 30 and 40 GeV. .

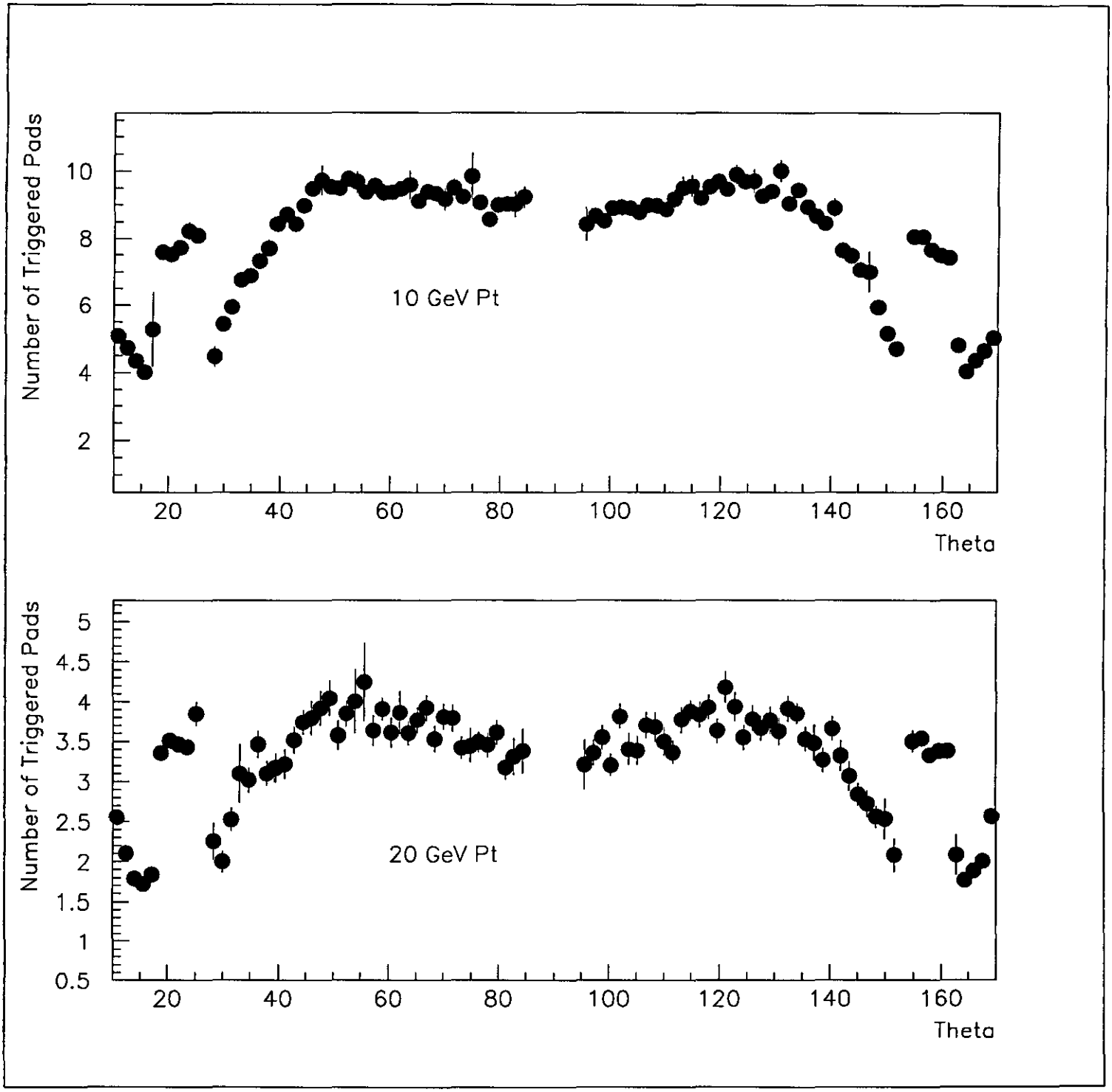

Figure 3a) Scan of the average value of the distribution of strips for the sagitta determination of a trigger road as a function of θ. These distributions are for a constant P_t of 10 and 20 GeV. .

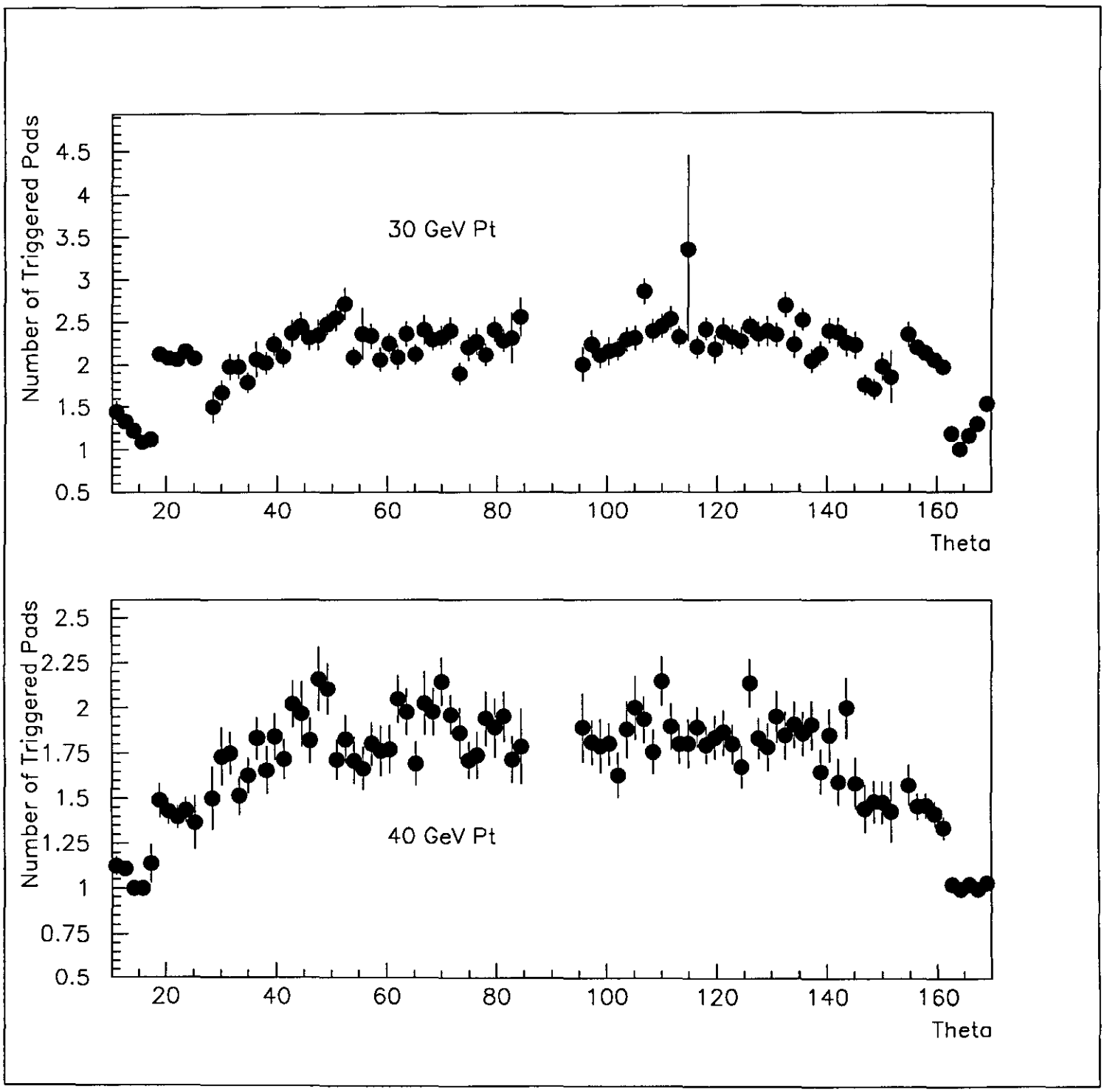

Figure 3b) Scan of the average value of the distribution of strips for the sagitta determination of a trigger road as a function of θ. These distributions are for a constant P_t of 30 and 40 GeV.

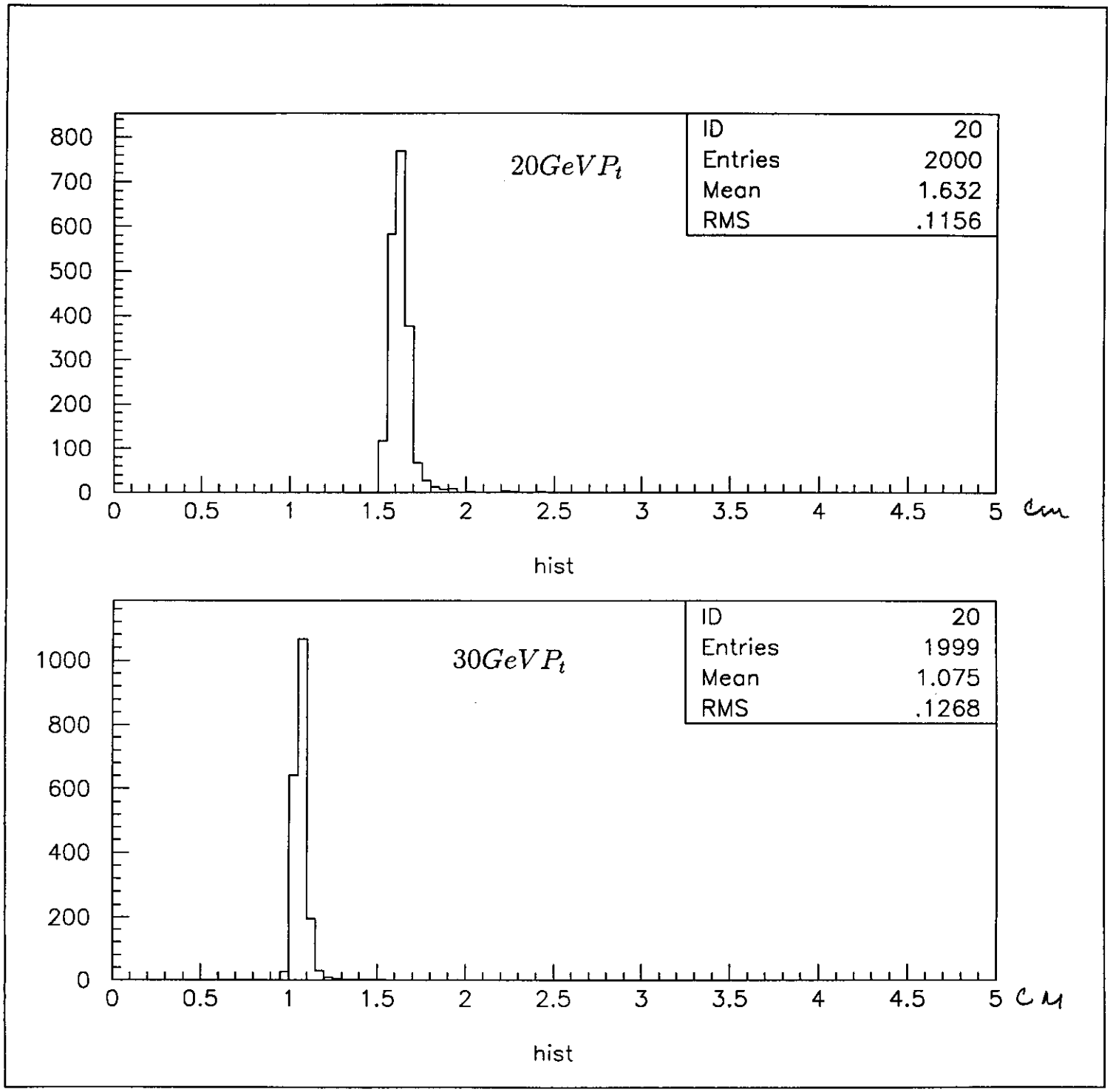

Figure 4a) These plots are the distribution of the sagitta in cm at $\theta = 20^0$ and at 20 and 30 GeV P_t respectively. No digitization has been done, these are plots of the physical parameter.

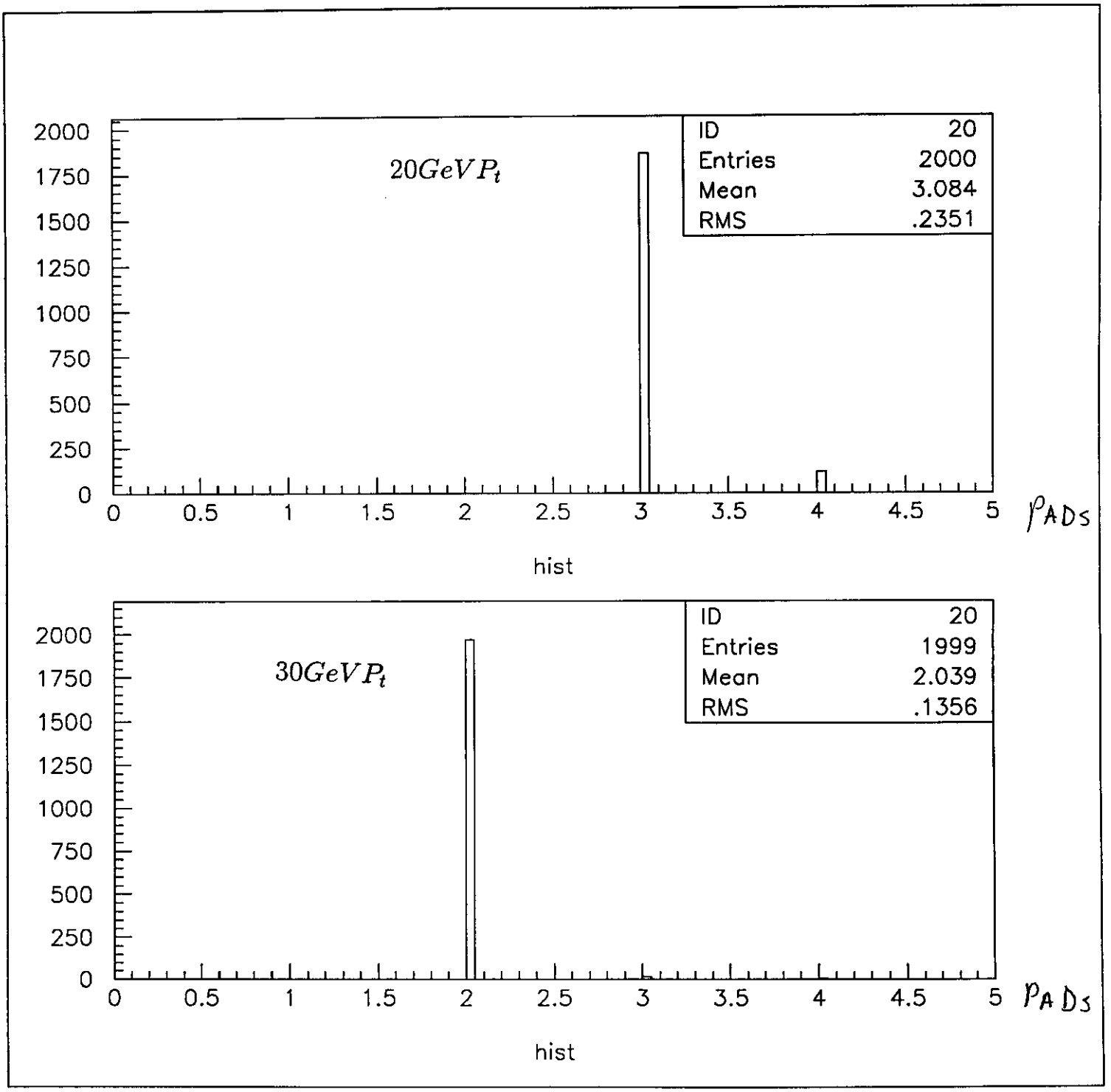

Figure 4b) In these plots the sagitta of figures 4a have been discriminated but not "digitized" as discribed in the text. Note that between 20 and 30 GeV at $\theta = 20^0$ the discriminated sagitta, i.e. number of strips assigned to the perfect determination of the positions used to measure the sagitta, there is only one strip difference in 20 and 30 GeV.

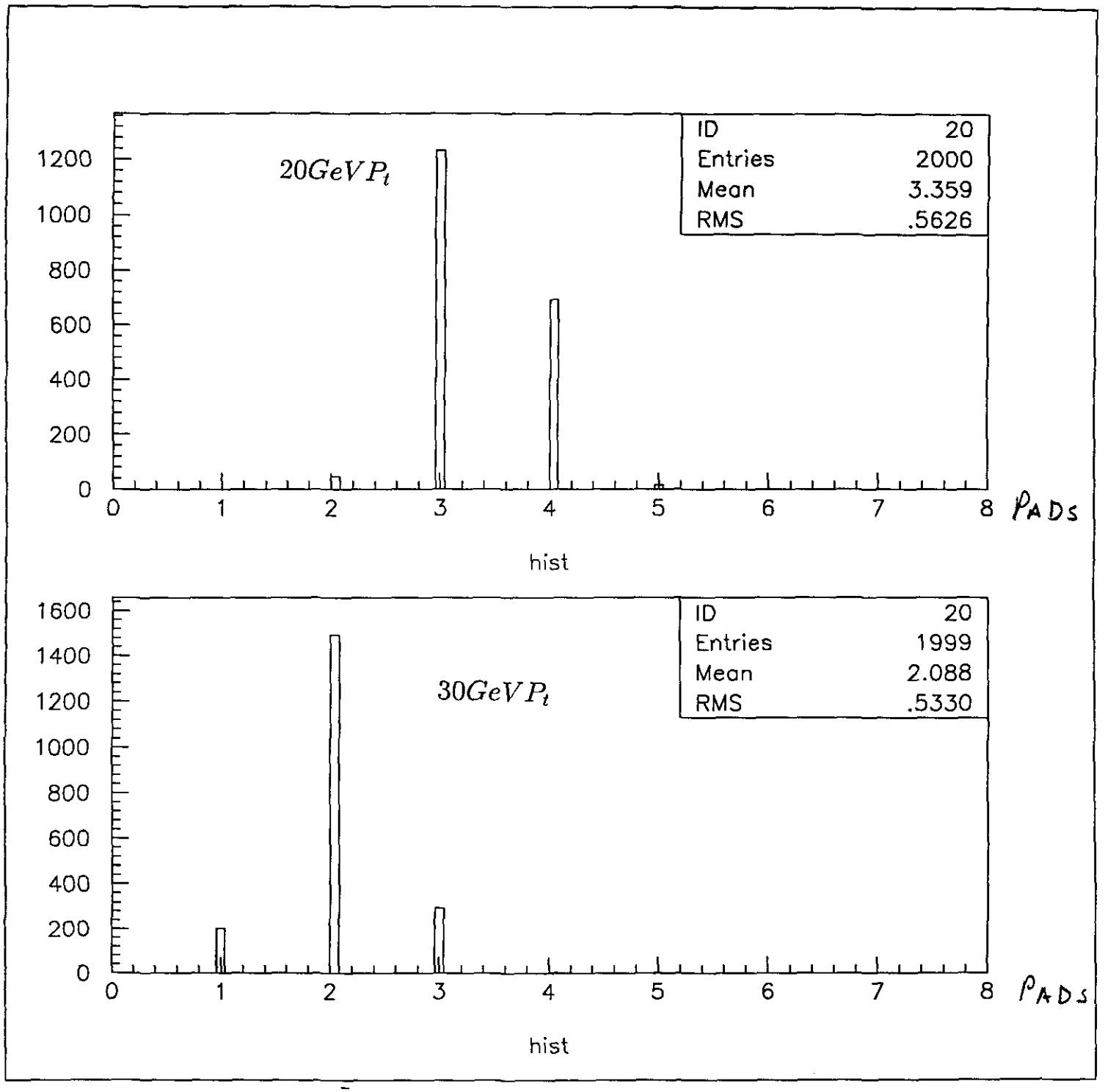

Figure 4c) In these plots the discriminated sagitta of figures 4b have been randomized in accordance with the distribution of charge induced on a strip. Note that there is significant overlap between 20 and 30 GeV at $\theta = 20^0$. About 20% of the events associated with 2 strips (30 GeV) now have 1 or 3 strips.

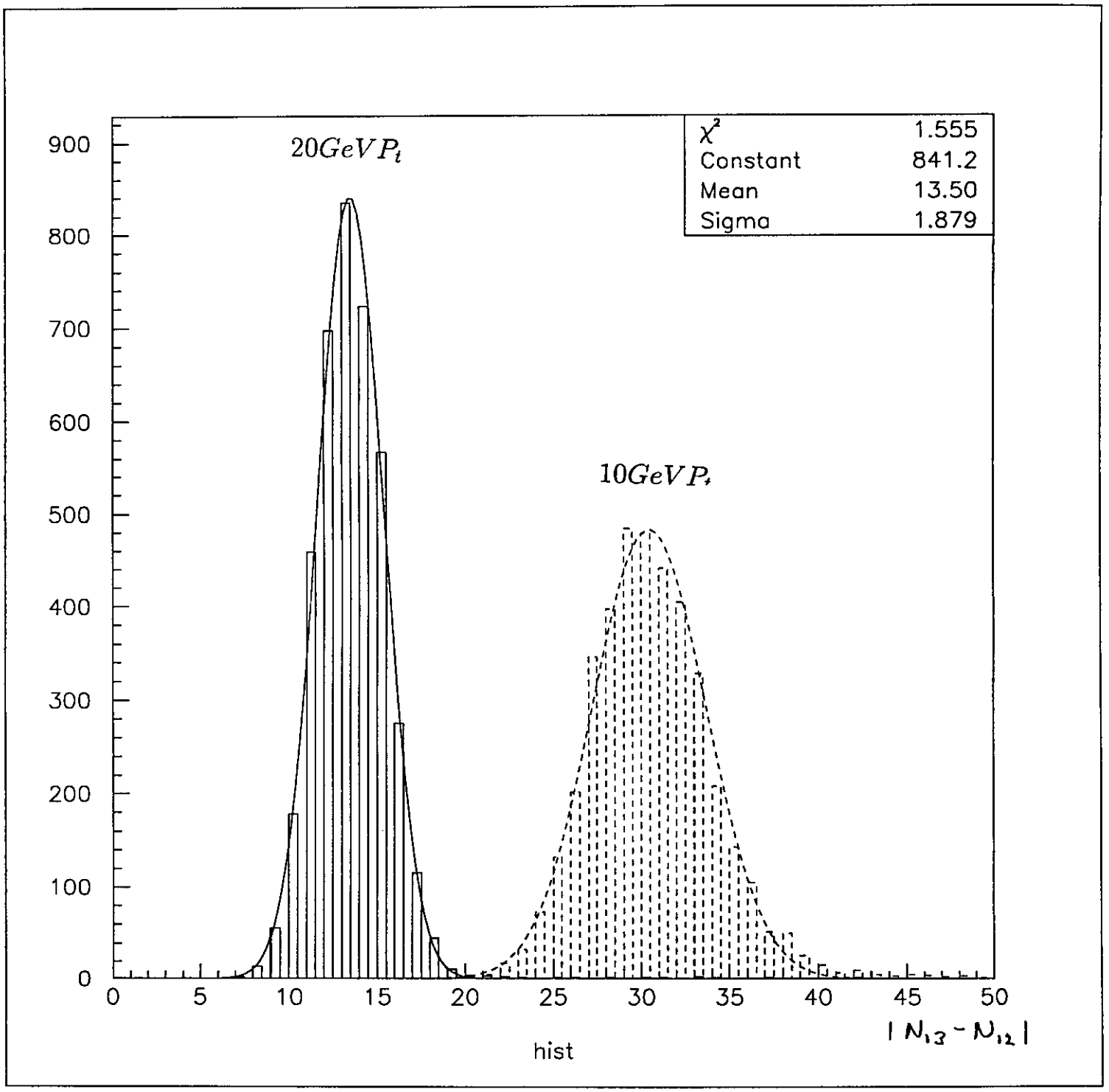

Figure 5) This plot shows the overlap in the barrel at $\theta = 80^0$ for the $\Delta\phi$ determination of the trigger road, for muons of 10 and 20 GeV P_t. In this plot the $\Delta\phi$ has been fully digitized.

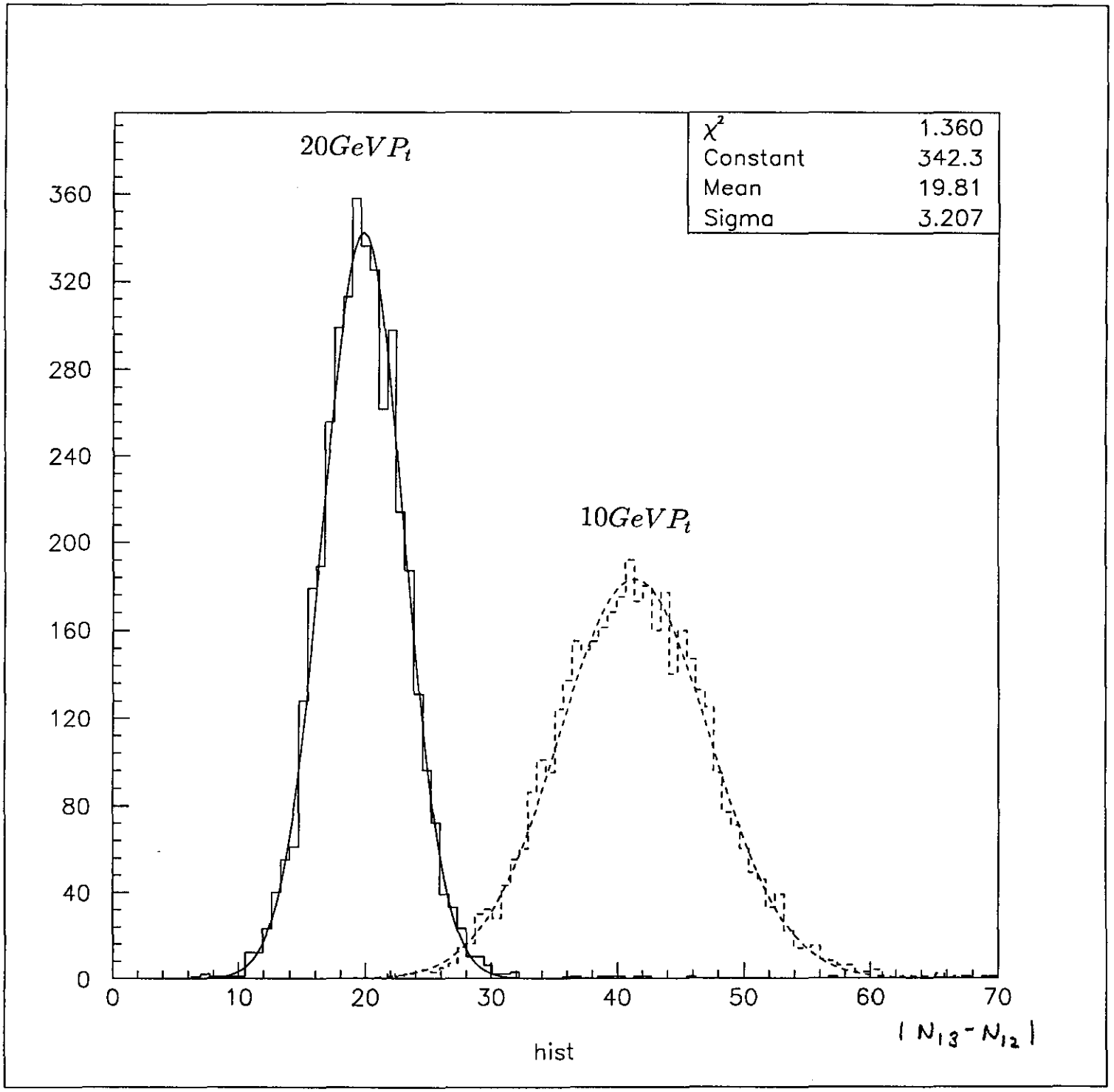

Figure 6a) This plot shows the overlap in the endcap at $\theta = 20^0$ for the $\Delta\phi$ determination of the trigger road, for muons of 10 and 20 GeV P_t. In this plot the $\Delta\phi$ has been fully digitized.

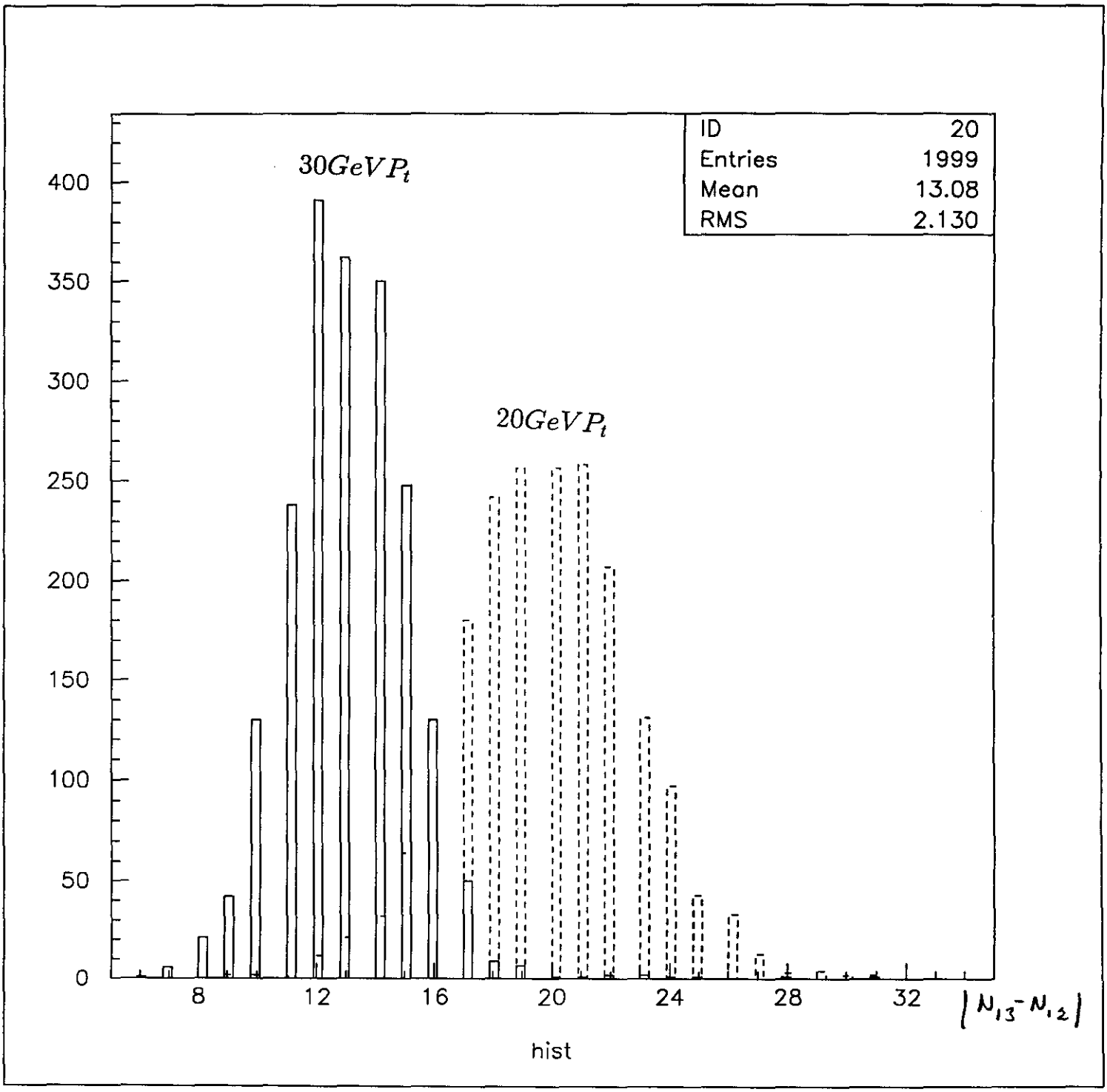

Figure 6b) This plot shows the overlap in the endcap at $\theta = 20^0$ for the $\Delta\phi$ determination of the trigger road, for muons of 20 and 30 GeV P_t. In this plot the $\Delta\phi$ has been fully digitized.

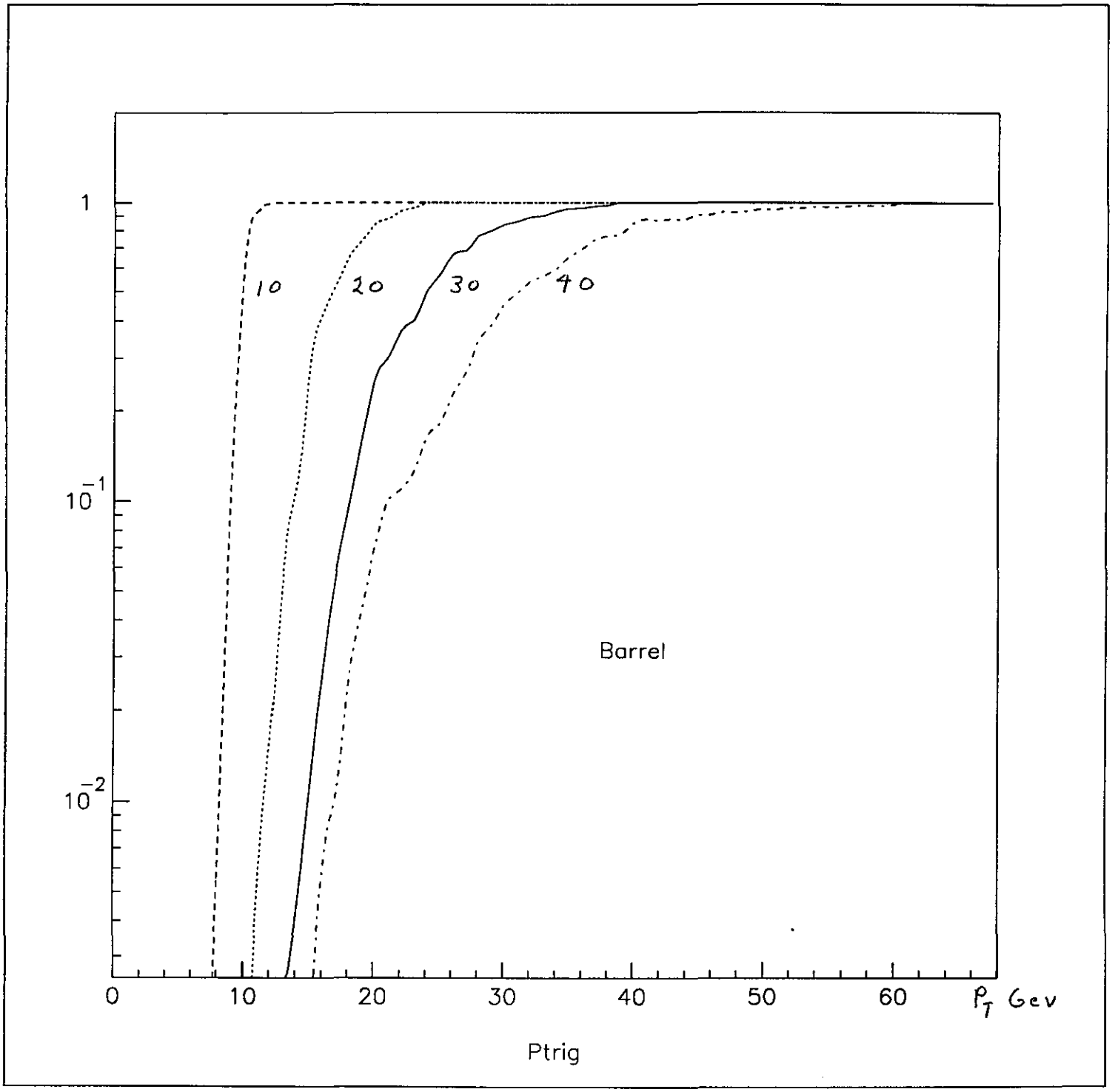

Figure 7) These plots show the trigger efficiency in the barrel muon system for trigger thresholds of 10, 20, 30, and 40 GeV P_t. The trigger efficiency is set, by design, to be $\sim 84\%$.

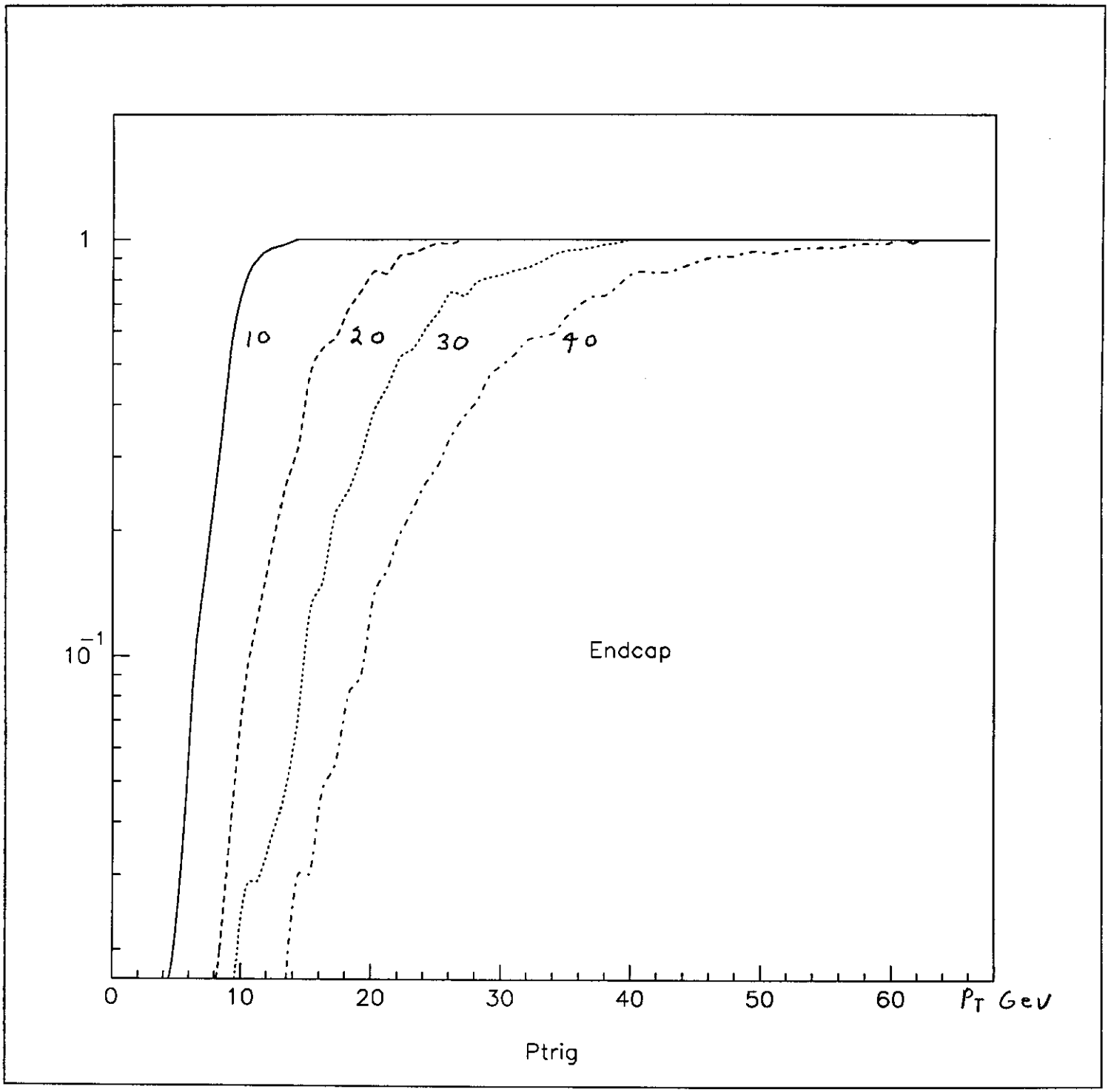

Figure 8) This plot shows the trigger efficiency in the endcap muon system for trigger thresholds of 10, 20, 30, and 40 GeV P_t. The trigger efficiency is set, by design, to be $\sim 84\%$.

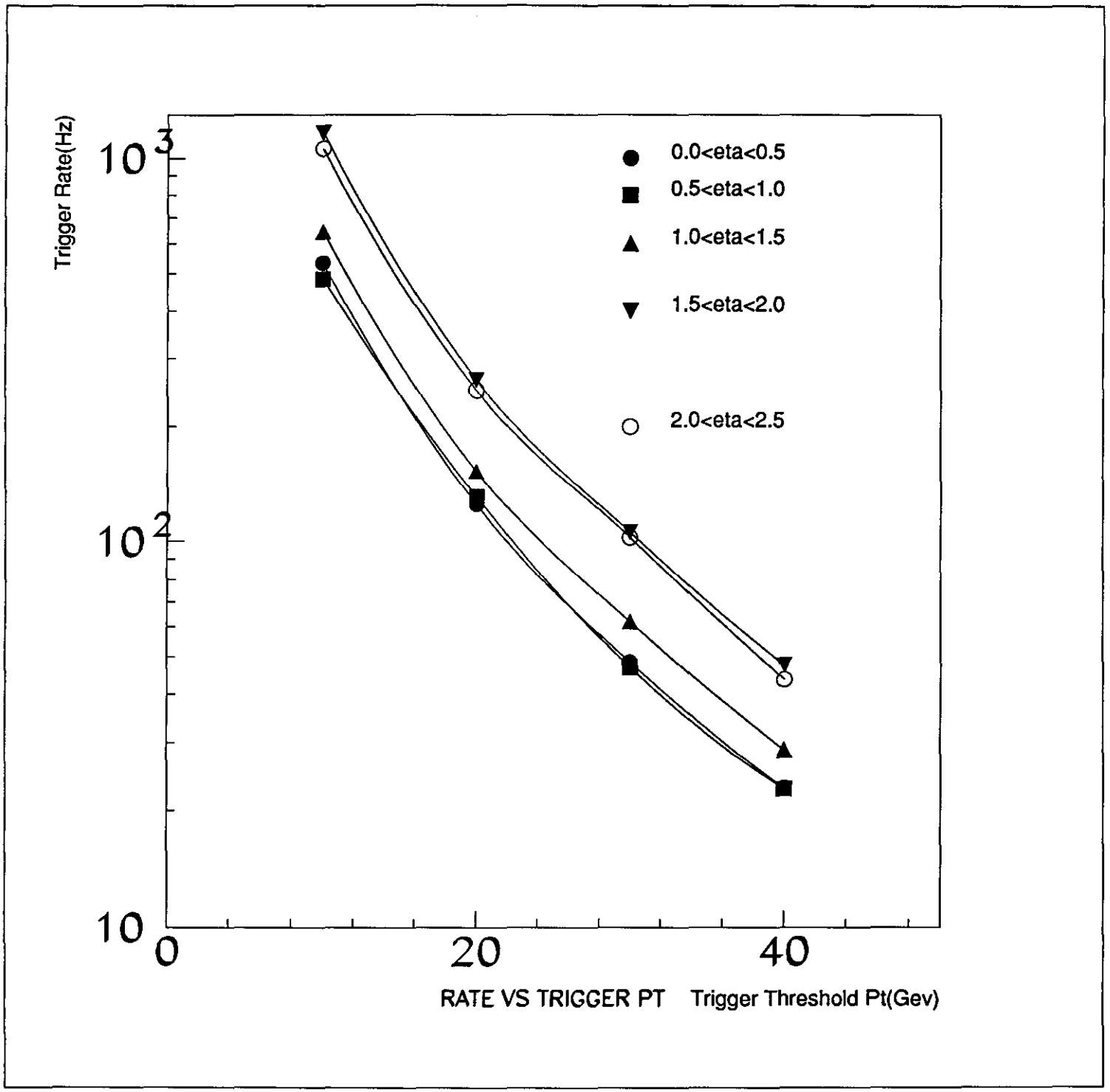

Figure 9) This plot shows the expected trigger rates as a function of P_t threshold for 4 different η bins. They were derived by the convolution of the trigger efficiencies with ISAJET TWOJET events as discribed in the text at a luminosity of $10^{33} cm^{-2} sec^{-1}$. .

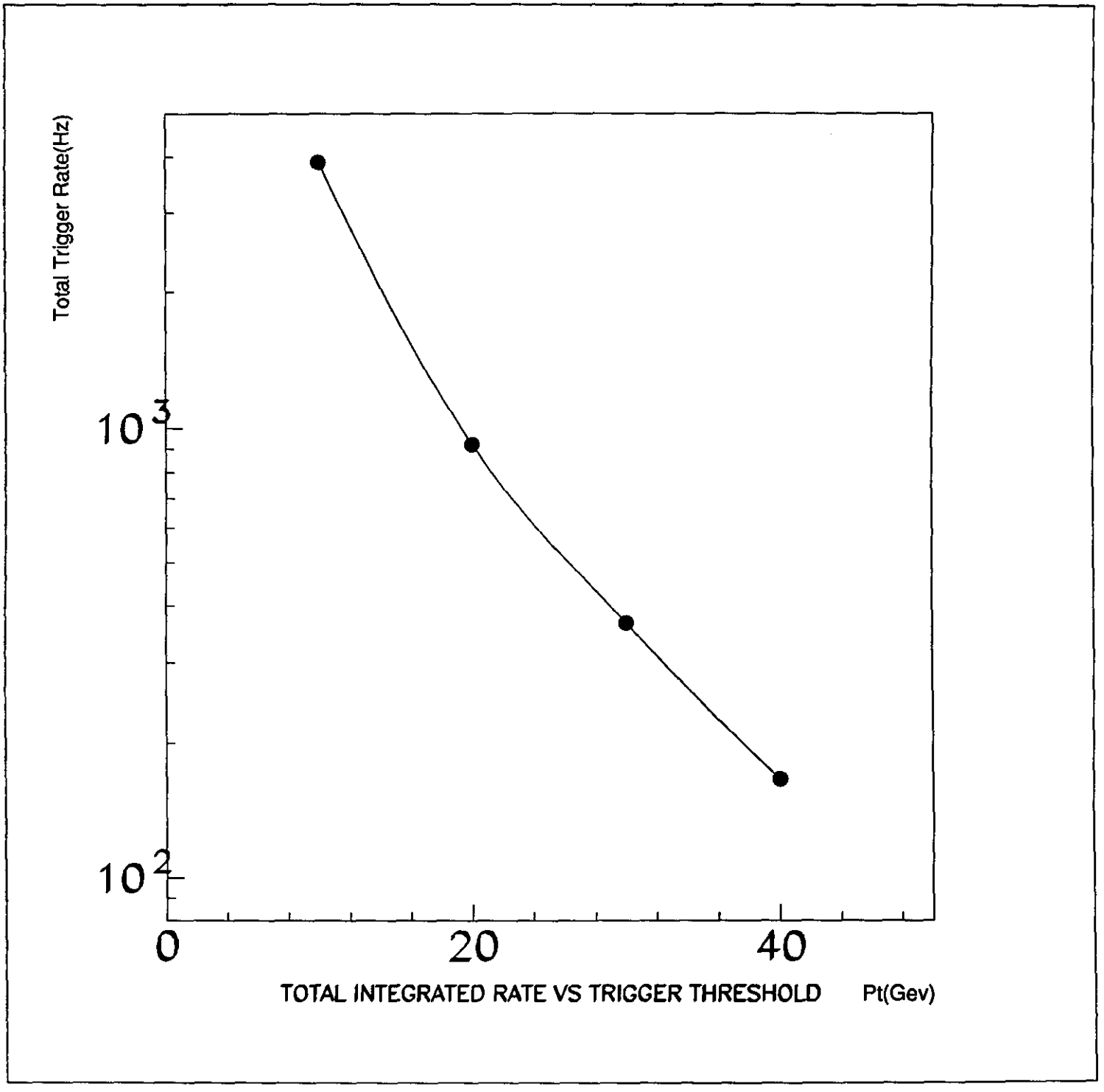

Figure 10) This plot shows the total integrated trigger rate as a function of the P_t threshold over the whole muon detector. The events are those described in the text and in the figure caption of figure 9.